Searching on the edge: dynamic oceanographic features increase foraging opportunities in a small pelagic seabird

Federico De Pascalis[1,*]**, David Pala**[2]**, Danilo Pisu**[2]**, Jennifer Morinay**[3]**,**
Andrea Benvenuti[4]**, Carmen Spano**[5]**, Alberto Ruiu**[5]**, Lorenzo Serra**[3]**,**
Diego Rubolini[1]**, Jacopo G. Cecere**[3]

[1]**Dipartimento di Scienze e Politiche Ambientali, Università degli Studi di Milano, 20133 Milano (MI), Italy**
[2]**Azienda Speciale Parco di Porto Conte, 07041 Alghero (SS), Italy**
[3]**Area Avifauna Migratrice, Istituto Superiore per la Protezione e la Ricerca Ambientale (ISPRA),**
40064 Ozzano dell'Emilia (BO), Italy
[4]**Ornis Italica, 00199 Rome (RM), Italy**
[5]**Area Marina Protetta Capo Caccia – Isola Piana, 07041 Alghero (SS), Italy**

ABSTRACT: Ocean mesoscale and submesoscale features, such as eddies and filaments, play a key role in the foraging ecology of marine predators, by concentrating nutrients and acting as aggregative structures for pelagic organisms. Highly pelagic seabirds may exploit these features to find profitable food patches in a dynamic and complex 3-dimensional spatial environment. Using miniaturized GPS loggers, we investigated whether foraging habitat selection of the Mediterranean storm petrel *Hydrobates pelagicus melitensis*, one of the smallest (ca. 28 g) seabirds worldwide, was affected by different static and dynamic oceanographic features during the breeding period. Individuals performed long foraging trips (up to 1113 km) in a relatively short time (1 to 2 d), covering large home ranges (up to 34 370 km^2), particularly during incubation. Different oceanographic features affected the at-sea distribution of storm petrels at different spatio-temporal scales. During incubation, individuals selected areas characterized by shallow waters and strong currents, conditions that may enhance vertical water mixing and increase food availability. During chick-rearing, they foraged closer to the colony, selecting shallow and productive areas, where increasing Lagrangian coherent structures and eddy kinetic energy enhanced foraging probability. These features could play an important role in storm petrels' foraging habitat selection, especially during chick-rearing, given their need to find predictable food patches in a short timespan. Overall, our results suggest that marine circulation processes are key drivers of the at-sea distribution of this small pelagic surface predator.

KEY WORDS: Ocean dynamics · Mesoscale features · Submesoscale features · Behaviour · Habitat selection · Storm petrel · Hidden Markov Model · *Hydrobates pelagicus melitensis*

1. INTRODUCTION

In seas and oceans, apex predators search for patchy and ephemeral food resources over large areas (Block et al. 2011). The marine realm is funda-mentally a turbulent system (Stewart 2008) where complex ocean dynamics move water masses (and therefore nutrients) in 3 dimensions, shaping the distribution of marine organisms (Haury et al. 1978, McManus & Woodson 2012, Bertrand et al. 2014).

Pelagic marine predators like seabirds can take advantage of such dynamicity, exploiting cues of the presence of food at different spatio-temporal scales (Fritz et al. 2003, Tew Kai & Marsac 2010, Scott et al. 2013). At the mesoscale extent (~100 km, weeks to months) for example, seabirds can predict the presence of productive areas (Weimerskirch 2007), likely exploiting features such as frontal regions and eddies (Schneider 1990, Cotté et al. 2007, Tew Kai & Marsac 2010, Scales et al. 2014). Eddies are turbulent spinning circulations, found almost everywhere in the ocean (Stewart 2008). They can enhance vertical fluxes of nutrients, increasing and modulating phytoplankton aggregations and structuring mesopelagic communities (Falkowski et al. 1991, Della Penna & Gaube 2020). Moreover, interactions between eddies generate, at their edges, strong dynamic interfaces that form submesoscale (<10 km, 1 to 10 d) structures of high biological activity (Lima et al. 2002) that seabirds may be able to track using visual/olfactory cues or atmospheric changes (Tew Kai et al. 2009). These structures, known as Lagrangian coherent structures (e.g. filaments, vortex boundaries, transport barriers), are of great ecological importance, not only because they are nutrient-enriched, but also because they aggregate plankton and marine propagules (Harrison et al. 2013) and have therefore strong bottom-up aggregative effects on higher trophic levels (Scales et al. 2018).

Procellariforms are seabirds with a highly pelagic lifestyle (Warham 1990) that rely on the ocean–atmosphere interface to find food resources, efficiently exploiting winds to fly with minimal metabolic costs across large distances through the so called 'dynamic soaring' flight (Richardson 2011, Richardson et al. 2018). Most procellariforms are surface feeders that exploit only the upper layer of the water column and have an extremely developed sense of smell, which is used to track different concentrations of dimethyl sulphide (an odorous compound released into the air by phytoplankton, especially when grazed by zooplankton), thereby finding profitable food patches over the ocean surface (Nevitt & Bonadonna 2005). Therefore, planktonic aggregative features such as eddies and Lagrangian coherent structures can be particularly important for procellariforms, which are likely to make use of a combination of olfactory and oceanographic cues at the (sub)mesoscale to locate areas where prey aggregate (Bastos et al. 2020)

We focused on one of the world's smallest (ca. 28 g; Cramp & Simmons 1977) procellariforms, the Mediterranean storm petrel *Hydrobates pelagicus meli-*

tensis (hereafter storm petrel). The planktivorous food habits and the olfactory ability of storm petrels (D'Elbée & Hémery 1998, Bonadonna & Sanz-Aguilar 2012, Bolton 2021) make them suitable candidates to investigate whether they exploit dynamic mesoscale and submesoscale features to locate profitable food patches. Using miniaturized GPS dataloggers, we tracked foraging trips of incubating (2020) and chick-rearing (2019) individuals from a colony in the Mediterranean Sea, a semi-enclosed basin characterized by an oligotrophic water regime with localized upwelling areas (Antoine et al. 1995, Casella et al. 2011). First, we described the movement patterns of breeding storm petrels. Second, we assessed the foraging habitat selection considering a range of oceanographic features at the meso- and submesoscale, accounting for the different effect of breeding stage/year. Different breeding stages are characterized by different spatio-temporal and energetic constraints (Shaffer et al. 2003). Typically, constraints are more relaxed during incubation than during chick-rearing, potentially leading birds to forage over broader areas. Indeed, incubating seabirds perform long-lasting foraging trips (up to 3 times longer than birds rearing chicks), travelling larger distances at greater range from the colony (Guilford et al. 2008, Ito et al. 2010, Sommerfeld & Hennicke 2010, Pinet et al. 2012), likely resulting in different features being exploited to locate food. Moreover, stage-specific nutritional requirements may lead individuals to exploit different food resources (Navarro et al. 2009), potentially resulting in stage-specific foraging habitat selection patterns. We expect meso- and submesoscale features to be key determinants of foraging behaviour, particularly during the more energy-demanding and time-constrained chick-rearing stage, when individuals have to minimize time at sea while maximizing foraging efficiency to regularly provide food to offspring, besides finding enough food for self-provisioning.

2. MATERIALS AND METHODS

2.1. General methods and GPS deployment

We GPS-tracked storm petrels breeding at the colony of Capo Caccia (Sardinia, Italy; 40° 35′ 18″ N, 8° 10′ 24″ E), hosting approximately 400 pairs (F. De Pascalis et al. unpubl. data) which nest both in rock crevices and on the ground of a marine cave. Birds were captured by hand while incubating their eggs or attending chicks and ringed with a unique metal

ring. We tagged 13 chick-rearing birds in July to August 2019 and 16 incubating birds in July to August 2020 (different individuals from those tracked in 2019). We deployed PathTrack (Otley) nanoFIX® GEO-MINI GPS loggers (ca. 0.9 g) set to record 1 fix every hour during incubation and 1 fix every 20 min during chick-rearing (accounting for the expected differences in trip duration during different breeding stages). Devices were attached to the basal section of 4 central tail feathers (being careful not to cover the uropygial gland papilla) using 2 to 3 thin (ca. 2 to 3 mm) strips of Tesa® tape (Tesa). Device relative weight (including attachments) was around 4% of bird body mass (incubation: 3.4%; chick-rearing: 4.4%). During incubation, we tagged only birds with eggs where the embryo was clearly visible but not fully grown (assessed by egg candling) to avoid tracking individuals that had just laid the egg or had clutches that were too close to hatching. During handling, the egg was covered with a wool layer to avoid heat dispersion. After handling, individuals were carefully placed back on their nests and covered for approximately 5 min to make them settle back. Chick-rearing birds were tagged only if the chick body mass was over 10 g (mean ± SD: 16.3 ± 6.2 g chick body mass from tracked birds) to avoid subjecting chicks to thermal stress when left alone by the captured parent. To minimize tracking duration, device retrieval started the second day following deployment during incubation and the first night during chick-rearing, aiming at obtaining a single foraging trip per individual. To minimize colony disturbance, we visited the colony for only 7 non-consecutive days (or nights during chick-rearing) after deployment. Individual body mass was recorded to the nearest 0.1 g before and after GPS deployment using an electronic scale, while standard morphometric measurements (including head–bill length [HBL], to the nearest 0.1 mm) were taken only at GPS retrieval. We recovered 12 (out of 16) devices during incubation and 11 (out of 13) during chick-rearing. During incubation, the 4 missing devices were from birds that abandoned their nest soon after capture and were not seen again. The 2 missing devices during chick-rearing were from birds that had likely returned only for a short period of time to feed the chick (that was seen alive) and were therefore missed. We decided not to attempt further device recovery to minimize disturbance to the colony. All the retrieved devices contained data obtained during incubation while only 7 contained data obtained during chick-rearing. We recorded 13 foraging trips during incubation and 9 during chick-

rearing, from a total of 19 individuals (see Fig. 1). Capture, handling and tagging procedures were carried out under the supervision of the Italian Institute for Environmental Protection and Research (ISPRA), under the authorization of Law 157/1992 (Art. 4[1] and Art. 7[5]), which regulates research on wild bird species, and with permission of Parco Naturale Regionale di Porto Conte. Given the small size of storm petrels and their sensitivity to disturbance, possible detrimental effects of GPS-deployment on 3 parameters (body mass, foraging trip duration, hatching success) were investigated (see Appendix for details). We found no direct evidence of a negative effect of device on these traits. The tracking dataset is available upon request on the BirdLife Seabird Tracking Database (www.seabird-tracking.org).

2.2. Foraging trip characterization and variation according to breeding stage

Foraging trips were visually identified using QGIS v2.18 (QGIS Development Team 2009). Spatial and temporal duplicates, as well as unrealistic fixes according to derived ground speed, were identified and removed from the dataset using the 'SDLfilter' R package (Shimada 2019). To homogenize sampling interval and to account for irregular sampling rate (particularly severe during 2019, when gaps were frequent; mean ± SD sampling rate, 2019: 36 ± 128 min, 2020: 67 ± 60 min), we linearly interpolated and re-sampled the dataset at 1 h intervals (both for incubation and chick-rearing) using the 'adehabitat-LT' R package (Calenge 2006). We then calculated, for each complete foraging trip (i.e. starting and ending at the colony, n = 20), the following spatio-temporal trip metrics: trip duration (h), total trip length (km), mean and maximum linear distance from the colony (km), mean and maximum linear distance from the nearest coast (km), and mean and maximum speed between subsequent steps (m s^{-1}).

The effect of breeding stage on variation in spatio-temporal trip metrics was assessed by means of different linear mixed models (LMMs) using the 'lme4' R package (Bates et al. 2015), including individual identity as a random intercept effect. Significance was tested by likelihood ratio tests. Mean and maximum distance from the coast were log$_{10}$-transformed to ensure normality of residuals. For each bird, we calculated individual home ranges (km^2) using kernel density estimation (KDE, 90% contours) from the 'KernSmooth' R package (Wand

2015). Optimized covariance bandwidth matrices were obtained using the least squares cross validator estimator from the 'ks' R package (Duong 2007) on projected coordinates, to prevent spatial biases. The effect of breeding stage on individual home range was tested using a linear model, after $\log_{10}$-transforming home range areas to improve normality of residuals. Cumulative (all individuals pooled together) 25, 50, 70 and 90% KDEs for the 2 breeding stages were computed to illustrate differences in spatial behaviour between incubation and chick-rearing. All model assumptions were inspected for each fitted model using the 'performance' R package (Lüdecke et al. 2020).

To assess if body condition affected foraging behaviour, we computed the scaled mass index (SMI) (Peig & Green 2009) for each individual. We calculated the SMI by scaling body mass at device deployment with HBL (distance between the back of the skull and the tip of the bill). HBL was positively correlated with body mass (r = 0.64, n = 17), resulting in the SMI for individual i being computed as: $SMI_i =$ body mass$_i$ × $(HBL_0/HBL_i)^{2.14}$, where $HBL_0 = 325.59$ mm (mean HBL of the sample population). We then calculated the Spearman's rank correlation coefficient between each trip metric and the SMI. In the case of multiple trips per individual, only the first trip was considered.

2.3. Identification of at-sea behaviours

We identified at-sea behaviours from tracking data by means of Hidden Markov Models (HMMs) using the 'momentuHMM' R package (McClintock & Michelot 2018). Before running models, trips that prior to interpolation had temporal gaps exceeding 3 h were identified and split into separate bursts (before and after the gap) to avoid affecting behavioural estimation. We ran a 2-state HMM using the Viterbi algorithm to estimate the most probable behavioural state sequence (Zucchini et al. 2017). The number of states was based on *a priori* knowledge of procellariform at-sea behaviour (Pohle et al. 2017) and took into account the coarse temporal resolution of data. Optimal prior selection was checked after comparing negative log-likelihood values of a set of candidate models (n = 50), run iteratively using a range of randomly selected priors with reasonable values. Data streams used in the model were step length (i.e. distance travelled, modelled with a Gamma distribution) and turning angle (i.e. change of direction, modelled with a Von Mises distribution).

2.4. Foraging habitat selection

To assess the foraging habitat selection of storm petrels, we compared environmental features associated with searching/foraging (use) to those associated with travelling (non-use) locations, which were identified with the HMMs (see Section 3.2). We then associated each location with the corresponding value of the following features that were likely to affect storm petrel foraging behaviour. (1) Chlorophyll *a* concentration (mg m^{-3}; temporal resolution: daily; spatial resolution: 0.04°) and (2) sea surface temperature (°C, hourly, 0.04°) were both accessed through the EU Copernicus Marine Service Information (www.copernicus.eu). (3) Sea depth (m, 0.01°) was obtained from a NOAA dataset using the 'marmap' R package (Pante et al. 2018) and (4) slope (°, 0.01°) was calculated using the 'raster' R package (Hijmans 2018). (5) Eddy kinetic energy (EKE; m^2 s^{-2}, daily, 0.125°) was derived from the sea surface height anomaly field based on the geostrophic relationship and commonly used, despite some limitations, as a direct measure of number and intensity of mesoscale eddies (Qiu & Chen 2010, Tew Kai & Marsac 2010, Ding et al. 2020). EKE was computed as

$$\frac{1}{2}\left(U_a^2 + V_a^2\right) \tag{1}$$

where U_a and V_a are the zonal and meridional horizontal velocity (altimetry derived) components of the geostrophic current (obtained from SSALTO/Duacs products available from the Copernicus repository; m s^{-1}, daily, 0.125°). We also considered (6) the absolute value of backward finite-size Lyapunov exponents (FSLE; d^{-1}, 0.04°) as a proxy of submesoscale Lagrangian coherent structures (Boffetta et al. 2001, d'Ovidio et al. 2004), available from CLS/CNES Aviso (www.aviso.altimetry.fr). FSLE is a Lagrangian diagnostic technique that measures dynamic structures, and ridges of FSLE identify Lagrangian coherent structures (Tew Kai et al. 2009). Finally, we considered (7) current speed (m s^{-1}, daily, 0.04°), calculated as:

$$\sqrt{U_b{}^2 + V_b{}^2} \tag{2}$$

where U_b and V_b are the zonal and meridional horizontal velocity components (derived from the physical component of the Mediterranean Forecasting System available from the Copernicus repository).

Binomial Generalized Additive Mixed Models (GAMMs) were then used to assess if the selected environmental variables predicted the probability of use vs. non-use. We used GAMMs to account for potential non-linear relations between probability of use and

environmental variables. Environmental variables were not collinear (variance inflation factors [VIFs] ≤1.5; Hair et al. 2010). Separate models were fitted for incubation and chick-rearing stages using the 'mgcv' R package (Wood 2019). The response variable was coded as 1 if the HMM-identified behaviour was 'searching/foraging' (use), and as 0 if it was 'travelling' (non-use). Cubic regression splines with shrinkage were used in the models to avoid over-fitting. Two full models were fitted, and only the response curves of variables strongly (p ≤ 0.05) influencing foraging behaviour were plotted. To account for temporal autocorrelation, an inherent characteristic of tracking data, the model incorporated an auto-regressive AR1 correlation structure applied to each individual foraging trip (random effect) at regularly spaced time steps. All analyses were carried out using R 3.5.1 (R Core Team 2018).

nearest coastline), directed towards the Liguro-Provençal Basin and the Balearic Islands (NW, W). In 2020, incubating storm petrels engaged in long-lasting foraging trips (50.8 ± 11.1 h; mean ± SD), travelling large distances (737.0 ± 217.3 km) at high speed (4.0 ± 0.9 m s^{-1}). Conversely, in 2019, chick-rearing individuals engaged in much shorter foraging trips (24.4 ± 12.3 h), travelling less (255.2 ± 155.4 km) at lower speed (2.63 ± 0.9 m s^{-1}) and remained closer to the colony compared to incubating birds (Table 1, Fig. 1). These differences resulted in individual home ranges being 3 times larger during incubation (2020) compared to chick-rearing (2019) (Table 1, Fig. 1). Inter-individual differences in body condition did not significantly covary with trip metrics ($|r_S|$ always ≤ 0.42, p ≥ 0.18; see Table S1 in the Supplement at www.int-res.com/articles/suppl/m668 p121_supp.pdf).

3. RESULTS

3.1. Foraging trip characteristics and variation according to breeding stage

Breeding storm petrels performed highly pelagic foraging trips (approximately 60 km away from the

3.2. Identification of at-sea behaviours

We interpreted the 2 states estimated by the HMM as proxies of the following behaviours: State 1, characterized by small step length and high angle concentration, identified locations likely associated with food searching and/or foraging; State 2, character-

Table 1. Differences in spatio-temporal trip metrics between 2 breeding stages of storm petrels. Differences were assessed by means of linear mixed effects models, with individual identity as a random intercept effect. Significance was tested by likelihood ratio tests. The effect of breeding stage (incubation, chick-rearing) on home range size (from the 90% kernel density estimation [KDE]) was assessed by means of a linear model. Values are mean ± SD and range (minimum–maximum values observed). Only complete trips were considered in these analyses (n = 20)

Trip metric	Incubation (n = 12 trips)	Chick-rearing (n = 8 trips)	χ^2	df	p
Trip duration (h)	50.8 ± 11.1 (40.0–70.0)	24.4 ± 12.3 (12.0–44.0)	9.4	1	0.002
Total trip length (km)	737.0 ± 217.3 (299.1–1112.9)	255.2 ± 155.4 (48.5–480.3)	14.9	1	<0.001
Maximum distance from colony (km)	297.6 ± 82.3 (166.7–406.2)	123.4 ± 69.4 (29.0–215.5)	13	1	<0.001
Mean distance from colony (km)	177.1 ± 58.7 (74.2–271.6)	85.4 ± 51.8 (24.8–271.6)	9.4	1	0.002
Maximum distance from coast (km)	129.0 ± 60.8 (38.7–211.2)	102.9 ± 55.3 (21.8–166.6)	1	1	0.3
Mean distance from coast (km)	58.0 ± 36.1 (15.9–124.4)	64.9 ± 35.2 (11.3–104.0)	0.1	1	0.78
Maximum speed (m s^{-1})	9.8 ± 2.0 (6.7–12.5)	7.38 ± 1.7 (4.5–9.8)	7.7	1	0.006
Mean speed (m s^{-1})	4.0 ± 0.9 (2.1–5.2)	2.63 ± 0.9 (1.1–4.1)	8.5	1	0.003
Home range size (km^2)[a]	16458 ± 10650 (3460–34370)	4835 ± 3535 (933–9320)	3.3[b]	1	0.002

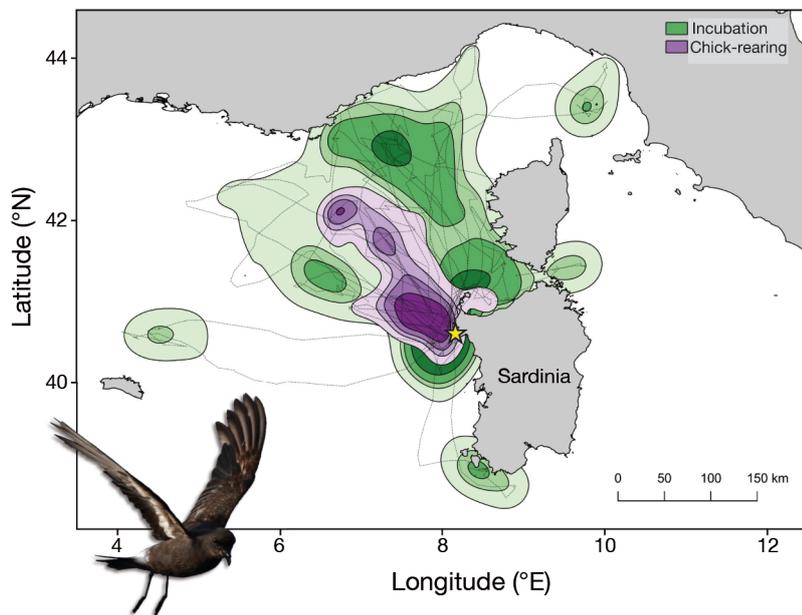[a]Incubation: n = 12; chick-rearing: n = 7 individuals; [b]t-value

Fig. 1. GPS tracks and cumulative kernel density estimates from breeding storm petrels. Kernel density estimates (25, 50, 70, 90% contours, from darker to lighter shades of colour) of incubating (2020, n = 12 individuals) and chick-rearing (2019, n = 7 individuals) storm petrels. (Dashed grey lines) GPS tracks; (★) colony location. Photo courtesy of Andrzej Tajchert

models). During incubation, foraging probability increased with decreasing sea depth (i.e. shallower waters) and current speed, and decreased with increasing temperature and FSLE (Fig. 3, model r^2 = 0.17). However, the association between foraging probability and FSLE was highly non-linear with large standard errors (Fig. 3c), implying a relatively weak pattern. During chick-rearing, a mixture of meso- and submesoscale dynamic oceanographic features, as well as biotic and static features, affected foraging behaviour of storm petrels (Fig. 4, model r^2 = 0.16). In particular, foraging probability increased with increasing EKE, FSLE (despite large standard errors for high FSLE values) and chlorophyll *a* concentration, and decreased with increasing sea depth.

4. DISCUSSION

Mediterranean storm petrels from our study population showed a highly pelagic lifestyle, as observed in previous studies (Bolton 2021, Rotger et al. 2020). They engaged in foraging trips of short duration (~1 or 2 d depending on the breeding stage) and travelled long distances (up to 1113 km), suggesting that the species has an extremely efficient flight performance as well as a high foraging efficiency. As commonly observed in procellariforms (e.g. Guilford et al. 2008, Cecere et al. 2013), breeding storm petrels travelled 3 times more and engaged in 2 times longer foraging trips during incubation compared to chick-rearing, when parents are more constrained to the nest by the need for frequent chick provisioning. Previous studies on the movement patterns of the species during breeding were conducted in the western Mediterranean waters (Rotger et al. 2020) and in the Atlantic Ocean (Bolton 2021). Differences in distance travelled and trip duration between populations during incubation were observed (Rotger et al. 2020: 73 h and 992 km; this study: 51 h and 737 km; Bolton 2021: 49 h and 562 km). Such differences could result from annual and individual variation, or reflect different energetic costs associated with different environments. Indeed, biotic (e.g. prey distribution) and abiotic (e.g. wind fields) factors can shape foraging costs for seabirds, affecting individual decision making (Afán et al. 2021).

ized by high step length and low angle concentration, likely corresponded to sustained travelling/relocation (Table 2, Fig. 2). For incubating birds in 2020, the proportion of searching/foraging locations per foraging trip was 0.60 ± 0.14 (mean ± SD) (n = 658), while it was 0.76 ± 0.15 for chick-rearing ones in 2019 (n = 183) (Mann-Whitney *U*-test; *W* = 50490, p < 0.001).

3.3. Foraging habitat selection

Different meso- and submesoscale features affected foraging habitat selection during the breeding period (see Figs. S1, S2 & S3 in the Supplement for the spatial distribution of the retained variables over different years and Table S2 for the output of full

Table 2. Parameters from the fitted 2-state Hidden Markov Model (HMM). Parameter estimates of step length and turning angle from the 2-state HMM with SD (concentration for turning angle) in parenthesis

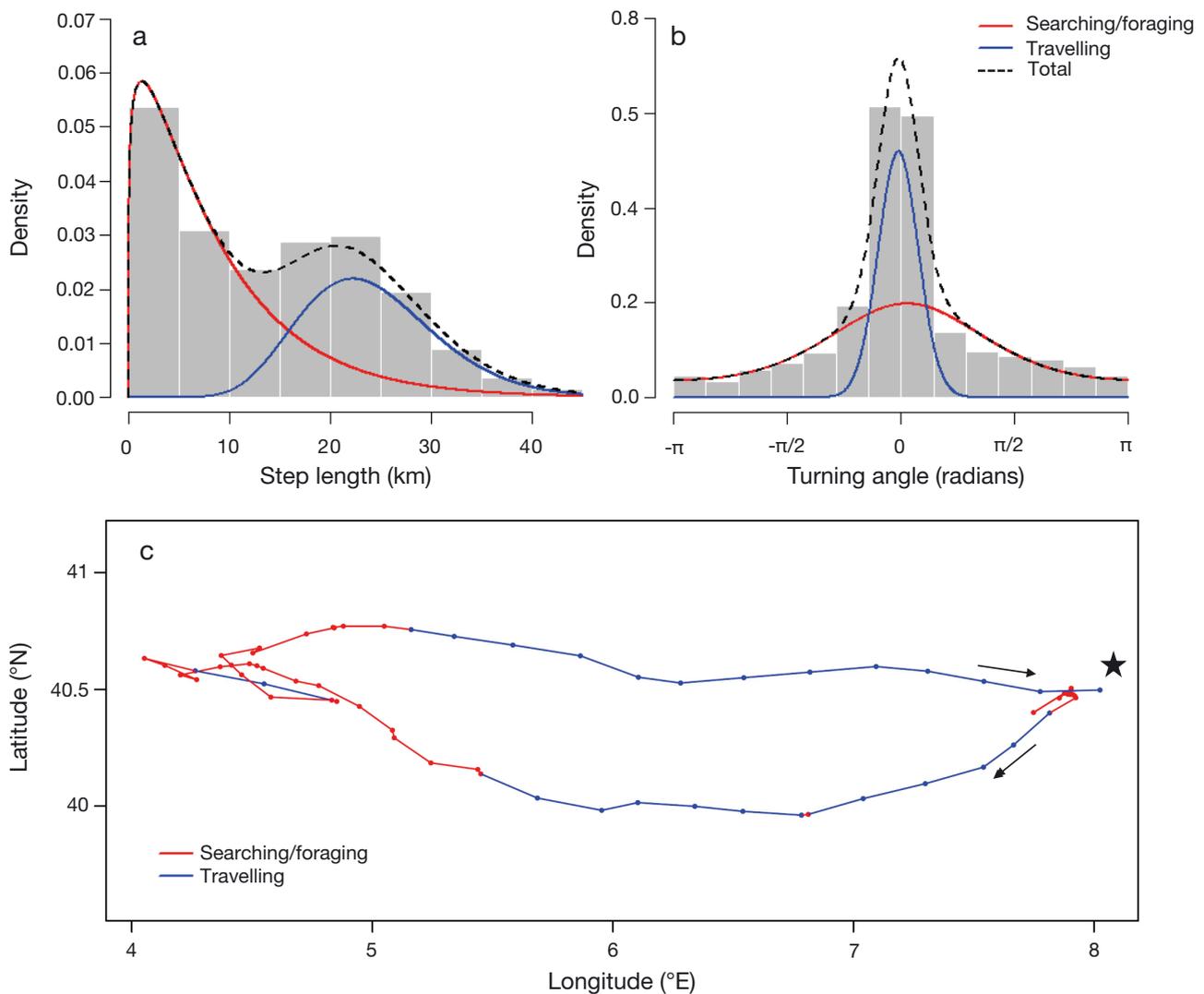| Parameter estimate	State 1 (searching/ foraging)	State 2 (travelling)
Step mean (km)	8.82 (8.06)	24.01 (6.69)
Turning angle mean (rad)	0.09 (0.81)	−0.03 (12.55)

Fig. 2. Probability distributions of behaviours estimated with a Hidden Markov Model (HMM) and example track. Density distributions of (a) step length and (b) turning angle in GPS data from 22 foraging trips of 19 storm petrels. Solid lines correspond to the estimated state-dependent probability distributions of the 2 identified behavioural states from the HMM. State 1: searching/foraging; State 2: travelling. (c) Example of a foraging trip coloured according to estimated underlying behaviours from the fitted HMM. (arrows) Trip direction; (★) colony location

Storm petrels foraged in areas characterized by water mixing and stirring, and their at-sea distribution was influenced by different oceanographic features. In 2020 (during incubation), foraging individuals selected areas characterized by cool and shallow waters and strong currents. The combined effect of strong currents and low sea depth (continental shelf or seamounts, for example) may increase vertical water mixing, generating upwelling and creating areas of elevated sub-surface primary production (Scott et al. 2010, Waggitt et al. 2018) or directly bringing zooplankton close to the sea surface. Similar dynamics have been observed for other plankti-vorous and/or surface-feeding seabirds in the ocean, where tidal currents interact with banks or shallow waters, increasing prey availability in the upper water layer (Hunt et al. 1998, Embling et al. 2012, Scott et al. 2013) (see Fig. S4 in the Supplement for further evidence supporting this combined effect). In 2019 (during chick-rearing), individuals concentrated on shallow and relatively more productive areas, with increasing EKE and FSLE values that are known to be associated with increased primary production and prey aggregation. Indeed, interactions between eddies and filamentation processes at eddy edges create packets of high biological activity, with
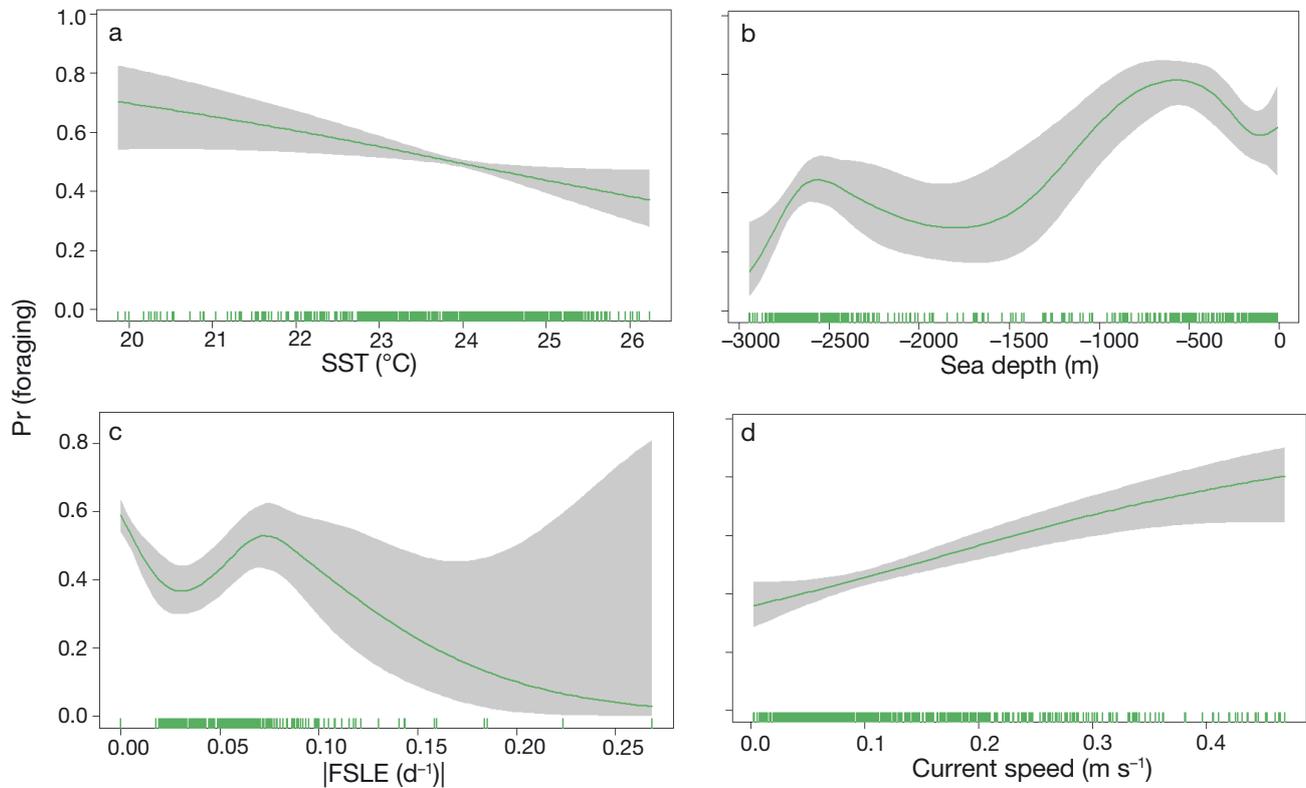
Fig. 3. GAMM response curves for key environmental predictors (p < 0.05) affecting foraging habitat selection of incubating storm petrels in 2020. Response curves (n = 12 trips) of the probability of foraging (0: non-use i.e. travelling, 268 fixes; 1: use i.e. searching/foraging, 390 fixes) according to (a) sea surface temperature (SST), (b) sea depth, (c) finite-size Lyapunov exponents (FSLE) and (d) current speed. Shaded areas correspond to the standard error of the estimate (green line), while ticks on the x-axis show the overall distribution of the data

marine larvae of different ages and origin clustered together in a small portion of the sea (Harrison et al. 2013). The observed differences between the 2 breeding stages may have multiple origins. Inter-annual differences in oceanographic features could influence the observed differences in habitat selection patterns (see Figs. S1–S3). In addition, the time constraints during chick-rearing likely promote the search for efficient proxies of prey availability, such as eddies and filaments, enabling individuals to quickly detect food resources close to the colony and be back at the nest, maintaining a positive energy balance. During incubation, individuals need to provision only for themselves, and they can roam over large areas opportunistically, looking for ephemeral but potentially highly rewarding prey aggregations, or even looking for other food sources that may not be available close to the colony (e.g. fishery discards, scavenging). Moreover, the different nutritional requirements of the 2 stages (chicks need highly energetic and lipid-rich food items; Wanless et al. 2005) could also promote the consumption of different prey

types occurring in different seascapes. Therefore, it is likely that a combination of different factors (i.e. year, breeding stage, foraging requirements) lead to the observed differences in foraging habitat selection between birds tracked in different breeding stages, and it is not possible to fully disentangle them. Regardless of these differences, we found that a set of static and dynamic oceanographic features at different spatio-temporal scales affected the at-sea distribution of foraging storm petrels. Such features increase the surface availability of prey, enabling this small predator to successfully forage even during periods of elevated energy demand. However, care must be taken in the interpretation of these results, given the small sample size and coarse GPS sampling rate. Finally, we point out that some other factors could affect storm petrel foraging decisions. Fishing vessels and fish farms could attract birds at sea, providing an alternative food source. Moreover, it is likely that wind speed and direction play a key role in foraging decision, restricting the search for food of this small-bodied species to specific locations and
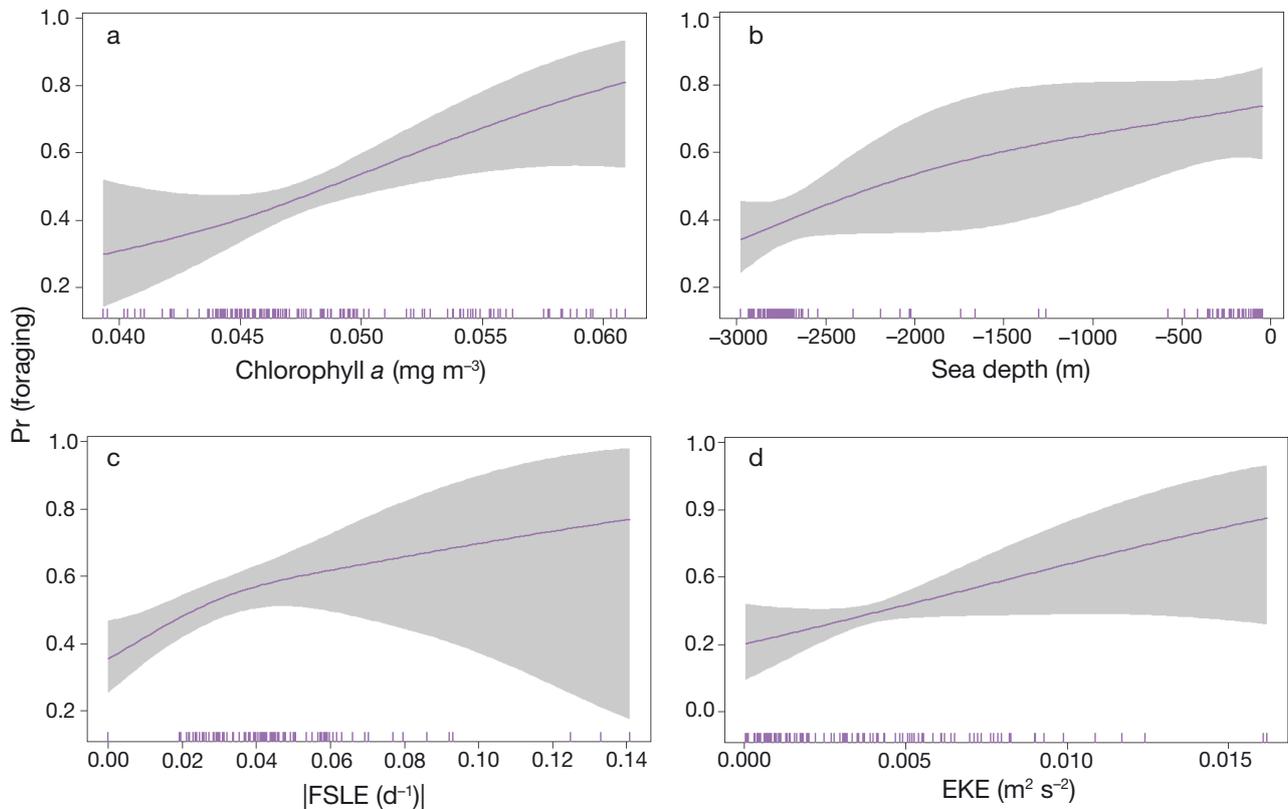
Fig. 4. GAMM response curves for key environmental predictors (p < 0.05) affecting foraging habitat selection of chick-rearing storm petrels in 2019. Response curves (n = 9 trips) of the probability of storm petrel foraging (0: non-use i.e. travelling, 45 fixes; 1: use i.e. searching/foraging, 138 fixes) according to (a) chlorophyll *a* concentration, (b) sea depth, (c) finite-size Lyapunov exponents (FSLE) and (d) eddy kinetic energy (EKE). Shaded areas correspond to the standard error of the estimate (purple line), while ticks on the *x*-axis show the overall distribution of the data

affecting the olfactory landscape and sea current formation (Nevitt 2008, Stewart 2008, De Pascalis et al. 2020). Therefore, an in-depth study investigating the energetic consequences of different wind conditions for the species is recommended.

Our results raise some pressing conservation concerns. The highly pelagic nature of this species during the breeding season (more than any other procellariform species breeding in the Mediterranean Sea; Louzao et al. 2006, Péron et al. 2013, 2018, Cecere et al. 2014), and the broad home ranges result in a wide range of threats encountered at sea. Such threats cannot be mitigated with area-based management, and require large-scale approaches (Oppel et al. 2018). Moreover, their tight foraging association with marine circulation processes (currents and eddies), coupled with surface-feeding constraints and a planktivorous diet, foster the risk of microplastic ingestion and bioaccumulation (Miller et al. 2020). Indeed, the central Mediterranean is highly contaminated by plastic debris, and microplastic movements and accumulation hotspots heavily depend on circu-

lation patterns (Guerrini et al. 2019, Caldwell et al. 2020). Broad-scale studies are needed to gain a better understanding of the species' at-sea ecology, in order to develop effective conservation plans at the entire Mediterranean scale. Given the importance of storm petrel foraging grounds for marine predators of different taxa (e.g. large pelagic fish and cetaceans; Notarbartolo di Sciara et al. 2003, Royer et al. 2004, Cotté et al. 2011), such conservation efforts will likely have top-down effects on whole trophic webs, enhancing across-taxa conservation in one of the most degraded marine ecosystems worldwide (Claudet & Fraschetti 2010).

della Tutela del Territorio e del Mare (PNM n. 28399 del 10/10/2019 - Gestione dei Siti di Interesse Comunitario/Zone Speciali di Conservazione che ricadono all'interno delle Aree Marine Protette).

LITERATURE CITED

Afán I, Arcos JM, Ramírez F, García D and others (2021) Where to head: environmental conditions shape foraging destinations in a critically endangered seabird. Mar Biol 168:23

Antoine D, Morel A, André JM (1995) Algal pigment distribution and primary production in the eastern Mediterranean as derived from coastal zone color scanner observations. J Geophys Res 100:16193–16209

Barron DG, Brawn JD, Weatherhead PJ (2010) Meta-analysis of transmitter effects on avian behaviour and ecology. Methods Ecol Evol 1:180–187

Bastos R, Martins B, Cabral JA, Ceia FR and others (2020) Oceans of stimuli: an individual-based model to assess the role of olfactory cues and local enhancement in seabirds' foraging behaviour. Anim Cogn 23:629–642

Bates D, Mächler M, Bolker BM, Walker SC (2015) Fitting linear mixed-effects models using lme4. J Stat Softw 67:1–48

Bertrand A, Grados D, Colas F, Bertrand S and others (2014) Broad impacts of fine-scale dynamics on seascape structure from zooplankton to seabirds. Nat Commun 5:5239

Blackmer AL, Ackerman JT, Nevitt GA (2004) Effects of investigator disturbance on hatching success and nest-site fidelity in a long-lived seabird, Leach's storm-petrel. Biol Conserv 116:141–148

Block BA, Jonsen ID, Jorgensen SJ, Winship AJ and others (2011) Tracking apex marine predator movements in a dynamic ocean. Nature 475:86–90

Boffetta G, Lacorata G, Redaelli G, Vulpiani A (2001) Detecting barriers to transport: a review of different techniques. Physica D 159:58–70

Bolton M (2021) GPS tracking reveals highly consistent use of restricted foraging areas by European storm-petrels *Hydrobates pelagicus* breeding at the largest UK colony: implications for conservation management. Bird Conserv Int 31:35–52

Bonadonna F, Sanz-Aguilar A (2012) Kin recognition and inbreeding avoidance in wild birds: the first evidence for individual kin-related odour recognition. Anim Behav 84:509–513

Caldwell J, Muff LF, Pham CK, Petri-Fink A, Rothen-Rutishauser B, Lehner R (2020) Spatial and temporal analysis of meso- and microplastic pollution in the Ligurian and Tyrrhenian Seas. Mar Pollut Bull 159:111515

Calenge C (2006) The package 'adehabitat' for the R software: a tool for the analysis of space and habitat use by animals. Ecol Model 197:516–519

Casella E, Molcard A, Provenzale A (2011) Mesoscale vortices in the Ligurian Sea and their effect on coastal upwelling processes. J Mar Syst 88:12–19

Cecere JG, Catoni C, Maggini I, Imperio S, Gaibani G (2013) Movement patterns and habitat use during incubation and chick-rearing of Cory's shearwaters (*Calonectris diomedea diomedea*) (Aves: Vertebrata) from Central Mediterranean: influence of seascape and breeding stage. Ital J Zool 80:82–89

Cecere JG, Gaibaniv G, Imperio S (2014) Effects of environmental variability and offspring growth on the move-

ment ecology of breeding Scopoli's shearwater *Calonectris diomedea*. Curr Zool 60:622–630

Claudet J, Fraschetti S (2010) Human-driven impacts on marine habitats: a regional meta-analysis in the Mediterranean Sea. Biol Conserv 143:2195–2206

Cotté C, Park YH, Guinet C, Bost CA (2007) Movements of foraging king penguins through marine mesoscale eddies. Proc R Soc B 274:2385–2391

Cotté C, D'Ovidio F, Chaigneau A, Lévy M, Taupier-Letage I, Mate B, Guinet C (2011) Scale-dependent interactions of Mediterranean whales with marine dynamics. Limnol Oceanogr 56:219–232

Cramp S, Simmons K (1977) The birds of the Western Palearctic. Oxford University Press, Oxford

D'Elbée J, Hémery G (1998) Diet and foraging behaviour of the British Storm Petrel *Hydrobates pelagicus* in the Bay of Biscay during summer. Ardea 86:1–10

d'Ovidio F, Fernández V, Hernández-García E, López C (2004) Mixing structures in the Mediterranean Sea from finite-size Lyapunov exponents. Geophys Res Lett 31: L17203

De Pascalis F, Collins PM, Green JA (2018) Utility of time-lapse photography in studies of seabird ecology. PLOS ONE 13:e0208995

De Pascalis F, Imperio S, Benvenuti A, Catoni C, Rubolini D, Cecere JG (2020) Sex-specific foraging behaviour is affected by wind conditions in a sexually size dimorphic seabird. Anim Behav 166:207–218

Della Penna A, Gaube P (2020) Mesoscale eddies structure mesopelagic communities. Front Mar Sci 7:454

Ding M, Lin P, Liu H, Hu A, Liu C (2020) Lagrangian eddy kinetic energy of ocean mesoscale eddies and its application to the Northwestern Pacific. Sci Rep 10:12791

Duong T (2007) ks: Kernel density estimation and kernel discriminant analysis for multivariate data in R. J Stat Softw 21:1–16

Embling CB, Illian J, Armstrong E, van der Kooij J, Sharples J, Camphuysen KCJ, Scott BE (2012) Investigating fine-scale spatio-temporal predator–prey patterns in dynamic marine ecosystems: A functional data analysis approach. J Appl Ecol 49:481–492

Falkowski PG, Ziemann D, Kolber Z, Bienfang PK (1991) Role of eddy pumping in enhancing primary production in the ocean. Nature 352:55–58

Fritz H, Said S, Weimerskirch H (2003) Scale-dependent hierarchical adjustments of movement patterns in a long-range foraging seabird. Proc R Soc B 270:1143–1148

Guerrini F, Mari L, Casagrandi R (2019) Modeling plastics exposure for the marine biota: risk maps for fin whales in the Pelagos Sanctuary (North-Western Mediterranean). Front Mar Sci 6:299

Guilford TC, Meade J, Freeman R, Biro D and others (2008) GPS tracking of the foraging movements of Manx shearwaters *Puffinus puffinus* breeding on Skomer Island, Wales. Ibis 150:462–473

Hair J, Black W, Babin B, Anderson R (2010) Multivariate data analysis: a global perspective. Pearson Education, London

Harrison CS, Siegel DA, Mitarai S (2013) Filamentation and eddy–eddy interactions in marine larval accumulation and transport. Mar Ecol Prog Ser 472:27–44

Haury LR, McGowan JA, Wiebe PH (1978) Patterns and processes in the time-space scales of plankton distributions. In: Steele JH (ed) Spatial pattern in plankton communities. Springer, Berlin, p 277–327

Heggøy O, Christensen-Dalsgaard S, Ranke PS, Chastel O, Bech C (2015) GPS-loggers influence behaviour and physiology in the black-legged kittiwake *Rissa tridactyla*. Mar Ecol Prog Ser 521:237–248

Hijmans RJ (2018) raster: geographic data analysis and modeling. https://cran.r-project.org/package=raster

Hunt GL Jr, Russell RW, Coyle KO, Weingartner T (1998) Comparative foraging ecology of planktivorous auklets in relation to ocean physics and prey availability. Mar Ecol Prog Ser 167:241–259

Ito M, Takahashi A, Kokubun N, Kitaysky AS, Watanuki Y (2010) Foraging behavior of incubating and chick-rearing thick-billed murres *Uria lomvia*. Aquat Biol 8:279–287

Lima ID, Olson DB, Doney SC (2002) Biological response to frontal dynamics and mesoscale variability in oligotrophic environments: Biological production and community structure. J Geophys Res C Oceans 107:3111

Louzao M, Hyrenbach KD, Arcos JM, Abelló P, Gil De Sola L, Oro D (2006) Oceanographic habitat of an endangered Mediterranean procellariiform: implications for marine protected areas. Ecol Appl 16:1683–1695

Lüdecke D, Makowski D, Waggoner P (2020) performance: assessment of regression models performance. https://cran.r-project.org/package=performance

McClintock BT, Michelot T (2018) momentuHMM: R package for generalized hidden Markov models of animal movement. Methods Ecol Evol 9:1518–1530

McManus MA, Woodson CB (2012) Plankton distribution and ocean dispersal. J Exp Biol 215:1008–1016

Miller ME, Hamann M, Kroon FJ (2020) Bioaccumulation and biomagnification of microplastics in marine organisms: a review and meta-analysis of current data. PLOS ONE 15:e0240792

Navarro J, Louzao M, Igual JM, Oro D and others (2009) Seasonal changes in the diet of a critically endangered seabird and the importance of trawling discards. Mar Biol 156:2571–2578

Nevitt GA (2008) Sensory ecology on the high seas: the odor world of the procellariiform seabirds. J Exp Biol 211:1706–1713

Nevitt GA, Bonadonna F (2005) Sensitivity to dimethyl sulphide suggests a mechanism for olfactory navigation by seabirds. Biol Lett 1:303–305

Notarbartolo di Sciara G, Zanardelli M, Jahoda M, Panigada S, Airoldi S (2003) The fin whale *Balaenoptera physalus* (L. 1758) in the Mediterranean Sea. Mammal Rev 33:105–150

Oppel S, Bolton M, Carneiro APB, Dias MP and others (2018) Spatial scales of marine conservation management for breeding seabirds. Mar Policy 98:37–46

Pante E, Simon-Bouhet B, Irisson JO (2018) marmap: import, plot and analyze bathymetric and topographic data. https://cran.r-project.org/package=marmap

Peig J, Green AJ (2009) New perspectives for estimating body condition from mass/length data: the scaled mass index as an alternative method. Oikos 118:1883–1891

Péron C, Grémillet D, Prudor A, Pettex E and others (2013) Importance of coastal Marine Protected Areas for the conservation of pelagic seabirds: the case of Vulnerable yelkouan shearwaters in the Mediterranean Sea. Biol Conserv 168:210–221

Péron C, Authier M, Grémillet D (2018) Testing the transferability of track-based habitat models for sound marine spatial planning. Divers Distrib 24:1772–1787

Pinet P, Jaquemet S, Phillips RA, Le Corre M (2012) Sex-specific foraging strategies throughout the breeding season in a tropical, sexually monomorphic small petrel. Anim Behav 83:979–989

Pohle J, Langrock R, van Beest FM, Schmidt NM (2017) Selecting the number of states in hidden Markov models: pragmatic solutions illustrated using animal movement. J Agric Biol Environ Stat 22:270–293

QGIS Development Team (2009) QGIS Geographic Information System. Available from: http://qgis.osgeo.org

Qiu B, Chen S (2010) Interannual variability of the North Pacific Subtropical Countercurrent and its associated mesoscale eddy field. J Phys Oceanogr 40:213–225

R Core Team (2018) R: a language and environment for statistical computing. R Foundation for Statistical Computing, Vienna. www.r-project.org/

Richardson PL (2011) How do albatrosses fly around the world without flapping their wings? Prog Oceanogr 88:46–58

Richardson PL, Wakefield ED, Phillips RA (2018) Flight speed and performance of the wandering albatross with respect to wind. Mov Ecol 6:3

Rotger A, Sola A, Tavecchia G, Sanz-Aguilar A (2020) Foraging far from home: GPS-tracking of Mediterranean storm-petrels *Hydrobates pelagicus melitensis* reveals long-distance foraging movements. Ardeola 68:3–16

Royer F, Fromentin JM, Gaspar P (2004) Association between bluefin tuna schools and oceanic features in the western Mediterranean. Mar Ecol Prog Ser 269:249–263

Scales KL, Miller PI, Embling CB, Ingram SN, Pirotta E, Votier SC (2014) Mesoscale fronts as foraging habitats: composite front mapping reveals oceanographic drivers of habitat use for a pelagic seabird. J R Soc Interface 11:20140679

Scales KL, Hazen EL, Jacox MG, Castruccio F, Maxwell SM, Lewison RL, Bograd SJ (2018) Fisheries bycatch risk to marine megafauna is intensified in Lagrangian coherent structures. Proc Natl Acad Sci USA 115:7362–7367

Schneider DC (1990) Seabirds and fronts: a brief overview. Polar Res 8:17–21

Scott BE, Sharples J, Ross ON, Wang J, Pierce GJ, Camphuysen CJ (2010) Sub-surface hotspots in shallow seas: fine-scale limited locations of top predator foraging habitat indicated by tidal mixing and sub-surface chlorophyll. Mar Ecol Prog Ser 408:207–226

Scott BE, Webb A, Palmer MR, Embling CB, Sharples J (2013) Fine scale bio-physical oceanographic characteristics predict the foraging occurrence of contrasting seabird species; gannet (*Morus bassanus*) and storm petrel (*Hydrobates pelagicus*). Prog Oceanogr 117:118–129

Shaffer SA, Costa DP, Weimerskirch H (2003) Foraging effort in relation to the constraints of reproduction in free-ranging albatrosses. Funct Ecol 17:66–74

Shimada T (2019) SDLfilter: filtering satellite-derived locations. https://cran.r-project.org/package=SDLfilter

Sommerfeld J, Hennicke JC (2010) Comparison of trip duration, activity pattern and diving behaviour by Red-tailed Tropicbirds (*Phaethon rubricauda*) during incubation and chick-rearing. Emu 110:78–86

Stewart RH (2008) Introduction to physical oceanography. University of Texas Press, Austin, TX

Tew Kai E, Marsac F (2010) Influence of mesoscale eddies on spatial structuring of top predators' communities in the Mozambique Channel. Prog Oceanogr 86:214–223

Tew Kai E, Rossi V, Sudre J, Weimerskirch H and others (2009) Top marine predators track Lagrangian coherent structures. Proc Natl Acad Sci USA 106:8245–8250

Waggitt JJ, Cazenave PW, Howarth LM, Evans PGH, van der Kooij J, Hiddink JG (2018) Combined measurements of prey availability explain habitat selection in foraging seabirds. Biol Lett 14:20180348

Wand M (2015) KernSmooth: functions for kernel smoothing supporting Wand & Jones (1995). https://cran.r-project.org/package=KernSmooth

Wanless S, Harris MP, Redman P, Speakman JR (2005) Low energy values of fish as a probable cause of a major sea-bird breeding failure in the North Sea. Mar Ecol Prog Ser 294:1–8

Warham J (1990) The petrels: their ecology and breeding systems. A&C Black, London

Weimerskirch H (2007) Are seabirds foraging for unpredictable resources? Deep Sea Res II 54:211–223

Wood S (2019) mgcv: Mixed GAM Computation Vehicle with Automatic Smoothness Estimation. https://cran.r-project.org/package=mgcv

Zucchini W, MacDonald IL, Langrock R (2017) Hidden Markov models for time series: an introduction using R, 2nd edn. CRC Press, Boca Raton, FL

Appendix. Evaluating GPS device effect on storm petrels

We assessed the effects of GPS devices on breeding storm petrels checking for differences in (1) body mass, (2) foraging trip duration and (3) hatching success between tagged and control birds.

For a subset of birds (n = 13), for which the device was removed immediately after the foraging trip, we compared body mass change (g) between GPS deployment and retrieval using a paired *t*-test. However, we did not measure body mass from a group of control birds to reduce any additional disturbance, since storm petrels are very sensitive to disturbance and handling (Blackmer et al. 2004).

We compared foraging trip durations of tagged and control birds during incubation. One of the main detrimental effects of device loading observed on seabirds is an increase in the energetic costs associated with foraging trips, resulting in longer foraging trip duration (Barron et al. 2010, Heggøy et al. 2015). During incubation, we deployed 2 camera traps in front of 3 active nests (with eggs), set to take time-lapse pictures every 20 min. We carefully marked 1 individual for each nest with a small white dot on the back of the head (without removing the animal from the nest) and we calculated foraging trip duration of 6 individuals, following De Pascalis et al. (2018). Foraging trip durations of tracked and control birds were then compared using an LMM with bird identity included as a random intercept effect. Significance was tested by the likelihood ratio test.

During incubation, we visited the colony in late August (22) to check the hatching success of tracked (n = 16) and control (n = 40) nests, and we used Fisher's exact tests to check for differences between the 2 groups. Control nests were located in an undisturbed nesting chamber that was accessed only twice, to count nests and to check hatching success.

Individuals did not decrease body mass after returning from a foraging trip (mean ± SD; deployment: 28.9 ± 2.8 g; retrieval: 29 ± 2 g; paired-samples *t*-test, t_{12} = −0.08, p = 0.93). With time-lapse cameras, we recorded 9 foraging trips from 9 incubating birds. Durations did not differ between control and experimental foraging trips (mean ± SD; control: 44.3 ± 19.4 h, n = 9; experimental: 51.4 ± 11.3 h, n = 12; df = 1; χ^2 = 0.78; p = 0.38). We found no difference in hatching success between tracked (25%, n = 16) and control (28%, n = 40) nests (Fisher's exact test, p = 1, odds ratio = 0.89).

Overall, we did not find any direct evidence of a detrimental GPS effect on storm petrels, a reassuring result that should nonetheless be taken with care, due to the small sample sizes considered. Tagged birds did not show a decrease in body mass, nor show longer trip durations, and had a similar hatching success to the control group. However, GPS-tagging individuals in natural nesting sites is difficult and challenging. Birds nest in high numbers on the ground of small caves (up to 100 nests in a single chamber), and natural egg loss due to movement of other birds (eggs are moved and then lost in crevices) is relatively common (F. De Pascalis et al. unpubl. data). Indeed, the eggs of the 4 birds that abandoned their nest after GPS-tagging had disappeared, and handling could lead to a momentary nest abandonment shortly afterwards that results in the egg being moved by other birds. Therefore, extreme care must be taken when tracking storm petrels in natural breeding sites such as caves. Researchers should preferentially target experienced individuals not at an early stage of incubation and breeding in shielded corners of the colony, preferably far from other clusters of nests.